Integrin and glycocalyx mediated contributions to cell adhesion identified by single cell force spectroscopy

2010 J. Phys.: Condens. Matter 22 194101

(http://iopscience.iop.org/0953-8984/22/19/194101)

J. Phys.: Condens. Matter **22** (2010) 194101 (11pp) doi:10.1088/0953-8984/22/19/194101

Integrin and glycocalyx mediated contributions to cell adhesion identified by single cell force spectroscopy

D Boettiger[1,2,3] **and B Wehrle-Haller**[1]

[1] Department of Physiology and Metabolism, University of Geneva, Geneva, Switzerland
[2] Departments of Microbiology and Pharmacology, University of Pennsylvania, Philadelphia, PA, USA
[3] Institute of Medicine and Engineering, University of Pennsylvania, Philadelphia, PA, USA

Received 15 October 2009, in final form 7 February 2010
Published 26 April 2010
Online at stacks.iop.org/JPhysCM/22/194101

Abstract
The measurement of cell adhesion using single cell force spectroscopy methods was compared with earlier methods for measuring cell adhesion. This comparison provided a means and rationale for separating components of the measurement retract curve that were due to interactions between the substrate and the glycocalyx, and interactions that were due to cell surface integrins binding to a substrate-bound ligand. The glycocalyx adhesion was characterized by multiple jumps with dispersed jump sizes that extended from 5 to 30 μm from the origin. The integrin mediated adhesion was represented by the F_{max} (maximum detachment force), was generally within the first 5 μm and commonly detached with a single rupture cascade. The integrin peak (F_{max}) increases with time and the rate of increase shows large cell to cell variability with a peak ~50 nN s^{-1} and an average rate of increase of 75 pN s^{-1}. This is a measure of the rate of increase in the number of adhesive integrin–ligand bonds/cell as a function of contact time.

(Some figures in this article are in colour only in the electronic version)

1. Introduction

The ability of cells to adhere specifically to each other and to their extracellular matrix was essential for the evolution of multi-cellular animals (metazoans). Integrin family receptors are found in species from sponges (porifera) to man [1, 2]. These receptors are required to mediate the morphological development of the adult from the zygote, maintaining the tissue structure once it has formed, and to the repair of injuries [3, 4]. These processes involve not only the ability to form adhesive bonds between specific cell surface integrins and immobilized ligands, but also the ability to regulate this adhesion as cells migrate through a tissue or change their contact surfaces, as must occur during morphological changes in tissue development, or due to adding a new cell through mitosis. This regulation must occur not only at the cellular level but different parts of the cell must function differently. For example, during cell migration the leading edge and the trailing edge must behave differently [5]. Since the identification of integrins as adhesion receptors, efforts have been focused on understanding the mechanisms by which they are controlled, using the approaches of molecular biology and structural protein chemistry. These studies have focused on specialized integrins in platelets that mediate adhesion to the blood vessel wall to prevent blood loss, and integrins on leukocytes that mediate adhesion to blood vessel walls at sites of parasitic invasion and inflammation [6]. These appeared with the evolution of a closed circulatory system (vertebrates) for platelets and with a cellular immune system (higher vertebrates) for the leukocyte adhesion [2]. The basic regulatory problem in these cases is to take a cell that is circulating in the blood and prevent it from adhering, even in the presence of large excesses of ligand, until it is triggered by a cell signal. These signals can activate integrins by converting them from a resting to a ligand binding conformation, the affinity modulation model [7–9]. The molecular mechanisms that mediate this integrin activation process are understood in considerable detail [10, 11]. This process controls the initial ligand binding reaction by controlling the proportion of the cell surface integrins that are available to bind the ligand following

a molecular collusion. Although this model has been widely applied to all integrin regulation, the issues and processes involved in the morphological development of tissues and cell migration are very different from the issues involved in the control of initial cell attachment of platelets to the vessel wall. The cells are already adherent and spend their whole lifetime as adherent cells. The problem is one of regulating the adhesion spatially within the cell and quantitatively and qualitatively with respect to their neighbors. Of course, there needs to be a feedback so that the cell can sense its adhesions, and this can come from the signaling capacity of integrins [12–15]. This problem is more complex that the regulation of initial adhesion and is not well understood at this time. There are two reasons for this (at least). First, we need to be able to measure changes in the number of adhesive bonds in response to experimental manipulations. Second, the signaling problem is more than an issue of chemical modifications. Not all signals are chemical, forces can also transmit signals, and force signals can interface with chemical signals [13].

This fundamental problem underlies the need for the development of methods to measure the number of adhesive bonds. The objective of this study is to examine single cell force spectroscopy in the light of measurements made from other approaches. Most of the cell biology literature from 1984 to the present on integrin mediated adhesion depends on a plate and wash type assay, where cells are plated on a ligand-coated surface for a set time and then the non-adhering cells are washed off and the remaining cells counted [16]. A refinement of this assay uses centrifugation to separate the non-adhering cells rather than washing [17]; however, as discussed below, these assays give a qualitative rather than a quantitative result. The spinning disc assay was developed to get a more quantitative measure of cell adhesion and has shown a linear relationship between the force necessary to detach cells and the number of adhesive bonds [18–20]. Single cell force spectroscopy was an outgrowth of the single bond analyses that were carried out using either an atomic force microscope or laser tweezers [21] and substituted whole cells in the place of the purified receptors [22, 23]. A major objective of both the single bond and much of the single cell force spectroscopy in the field of adhesion receptors has been directed at measuring single bond rupture strengths [23]. However, when integrins form adhesive bonds to substrate-bound ligands, the integrin clusters [24–26]. The range of functions of these clusters remains to be determined, but this raises the possibility that the real adhesive unit is not a single integrin but a cluster of integrins that gain mutual bond stability from the cluster or the cytoplasmic integrin binding proteins that also concentrate at these sites [27].

2. Methods

2.1. Cells and materials

K562 cells were obtained from ATCC and maintained in D-MEM with 10% fetal calf serum as a suspension culture. Cells were centrifuged to remove the medium and resuspended in D-PBS containing both Mg^{++} and Ca^{++} with added 2 mM glucose. A small volume of cells was added to a spot on a TPP 35 mm culture dish in which a center circle was drawn and fibronectin 10 μg ml^{-1} (Invitrogen) was adsorbed for 30 min, followed by blocking of the whole plate with HI Human Serum Albumen (1% in 0.1 M $NaHCO_3$ buffer pH 8.6 inactivated for 30 min at 37 °C). Cell suspensions were used over periods up to 2 h.

2.1.1. Spinning disc. The method and basic results have been described previously [18–20]. Briefly, K562 cells normally grow in suspension. An aliquot of cells was washed with PBS (Phosphate buffered saline), resuspended in PBS with additions of $MgCl_2$, $CaCl_2$, glucose (2 mM), and an activating monoclonal antibody (TS2/16 or QE2E5, 10 μg ml^{-1}) (when required to convert the $\alpha5\beta1$ to the active conformation), and evenly dispersed on a fibronectin-coated coverslip. After an incubation period, the coverslip was spun in the spinning disc device. This device applies a hydrodynamic shear gradient to the cell population causing the detachment of cells where the shear stress on the cell exceeds the total strength of the bonds holding the cell on the fibronectin substrate. The mean shear stress for cell detachment is calculated from the inflection point of a sigmoid curve fit ($f = 1/(1 + \exp[b(\tau - \tau_{50})])$, where τ_{50} is the mean shear stress for cell detachment) to the plot of relative proportion of cells remaining as a function of shear stress. Extensive analysis has shown that there is a linear relationship between the ligand density and the cell detachment force, which can be calculated from the cell geometry and the shear stress [18, 19, 28]. Analysis and curve fitting were done using SigmaPlot 7.0.

2.1.2. Atomic force microscopy. AFM measurements were carried out using a CellHesion 200 (JPK instruments, Berlin) and the data were analyzed using the JPK software CellHesion v3.0. The AFM was mounted on a Zeiss Axiovert 100 microscope. CSC12 cantilevers (MicroMash, Estonia) were washed in 1 M or 9 M H_2SO_4, washed with buffer to neutralize them and coated for 30 min in biotinylated BSA (SIGMA A6043) 50 μg ml^{-1} in 100 mM Na_2CO_3 buffer pH 8.6, washed in PBS, treated for 30 min with streptavidin (SIGMA S4762) 10 μg ml^{-1} in PBS, washed and incubated for 30 min in biotinylated Concanavalin A (SIGMA C2272) 40 μg ml^{-1} in PBS, and washed with PBS. Substrates were generated using 20 μl of ligand at 20 μg ml^{-1} in Dulbecco's PBS-A, in a marked circle in the center of a 35 mm culture dish (TPP) for 30 min, washed and blocked with heat-inactivated BSA for 30 min. Each cantilever was calibrated before cell attachment using the protocols in the CellHesion 200 software; a range of spring constants 0.015–0.08 N m^{-1} was used. Cell capture was carried out using approach and retract speeds of 5 μm s^{-1}, contact force of 3 nN for a contact time of 20 s. The cell capture was made from the BSA-coated regions of the plate, the captured cell was moved to the fibronectin-coated region and a series of measurements were made using a contact force of 0.5 nN, approach and retract speeds of 5 μm s^{-1}, and a series of increasing contact times: 5 s, 10 s, 20 s, 40 s, 60 s, and then repeating the pattern.

2.1.3. Wash assay. K562 cells in Dulbecco's complete PBS were labeled with calceinAM and distributed into 96-well plates that had been coated with fibronectin @5 μg ml^{-1} in Dulbecco's PBS-A and blocked with 1% heat-inactivated BSA in PBS-A. Cells were allowed various times to adhere, and then washed three times with a 96-well plate washer to distribute equal flow to all wells. The number of cells was evaluated by the calcein fluorescence in a fluorescent plate reader (Dynatech).

2.1.4. Centrifugation assay. K562 cells in Dulbecco's complete PBS were labeled with calceinAM and distributed into 96-well plates that had been coated with fibronectin @5 μg ml^{-1} in Dulbecco's PBS-A and blocked with 1% heat-inactivated BSA in PBS-A. Cells were allowed various times to adhere, the wells filled with complete PBS and sealed with sealing tape, inverted and centrifuged. After centrifugation the tape was removed while the plate remained inverted to remove the non-adhering cells. The wells were refilled with buffer and the number of cells was evaluated by the calcein fluorescence in a fluorescent plate reader (Dynatech). The buoyant density of K562 cells was evaluated using a step gradient with different densities constructed from dilutions of Lymphoprep. Cells were added to the gradient and spun at 2000 rpm. The cells were at the 1.045 density interface. The force on the cells was computed from $F = ma$, where m is 0.045(volume of the cell) and a is 9.8 m s^{-2}.

2.1.5. Electron microscopy. K562 cells growing in suspension were washed twice with PBS-A, and pelleted by centrifugation. The pellets were processed and stained with ruthenium red according to published protocols [29].

3. Results and discussion

3.1. Current analytic approaches

Three general approaches have been applied to the study of cell adhesion for fibroblasts and other normally adherent cells (i.e. with the exception of circulating blood cells). Because the biological outcomes, adhesion strength and level of downstream signaling, are dependent on the number of adhesive integrin bonds, the discussion focuses on this issue.

3.1.1. Morphological analysis of the distribution of adhesion molecules, or adhesion associated molecules on the cell–substrate interface. When adherent cells are placed in suspension, integrin family adhesion receptors are generally randomly distributed on the surface. When the cells are placed on a ligand-coated surface (ligand for the expressed integrin), the integrins form into clusters as adhesive bonds are formed [30]. These patches of integrins have been shown to be the sites of adhesion to the substrate by using glass needles to detach these points and watching the cell retract like a tent when a tent-stake is removed [31]. Since these clusters are associated with cell adhesion, they have been used as markers for integrin binding to the substrate ligand. The integrin clusters generate focal adhesions by the recruitment of cytoplasmic proteins that bind either directly or indirectly to the cytoplasmic domain of the integrin clusters [32, 33]. More than 50 different proteins have been associated with these structures [34]. Vinculin is a prominent member of this group which binds indirectly to integrin through talin and has been used as a measure of integrin binding [35]. This approach involves the assumption that clustering of integrin is equivalent to binding of a ligand. While this may correlate generally with the number of adhesive bonds, a quantitative relationship has not been validated experimentally and the measurement is indirect. The preferred method to quantify integrin in clusters is direct fluorescent labeling of the molecules with GFP (green fluorescent protein). This involves insertion or addition of the DNA coding sequences for GFP into the coding sequence of the protein of interest [36]. Thus, the use of this data to generate models involves assumptions that are difficult to test experimentally.

3.1.2. Quantitative analysis of the proportion of the cells that attach to a ligand-coated surface. In these methods, the cells are detached, placed in suspension, and then plated on a ligand-coated surface (most commonly using 96-well culture plates). After a period of time to allow adhesion, the cells that have not attached are removed and the remaining cells counted [16, 37]. The discrimination between adherent and non-adherent cells is made either by washing the plate (hydrodynamic shear), or inverting the plate and centrifuging (figure 1(A)). Similar results were obtained for each method. These methods have been widely used in the biological literature and often data is presented for a single time and ligand coating density. If we treat the cell and substrate as the reactants, one expects the increase in adherent cells to follow (pseudo) first order reaction kinetics (used for the curve fits in figure 1(A)). The difference is that adhesion will involve a large number of adhesive bonds, so that the thermodynamic dissociation process of cell from substrate has a very low probability. Hence the on-rate, off-rate and equilibrium cannot be determined for the adhesion receptor–ligand bonds. Since the wash assay and the centrifugation assay give similar results, we have used the force from the centrifugation assay to estimate the forces exerted in separating the cells into adherent and non-adherent fractions. The force applied to a K562 cell was determined from the cell volume, buoyant density, and the centrifugal acceleration using $F = ma$. 205 g would generate a ~200 pN force on a K562 cell. Atomic force microscope measurement for the bond strength of the $\alpha5\beta1$ integrin–fibronectin bond using purified components is 30–35 pN [38]. Thus, the assay will discriminate between cells that have <5–10 adhesive bonds and cells that have >5–10 adhesive bonds. The K562 cells express ~10^5 cell surface $\alpha5\beta1$ integrins [18]. If 25% are in the cell–substrate interface (the K562 cell spreads on the ligand-coated substrate to approximately the diameter of the cell in suspension), there would be 2.5×10^4 $\alpha5\beta1$ integrins available to bind. Although this assay has been very useful as a qualitative assay to identify receptors and ligands, it cannot discriminate between 10, and 10 000 adhesive bonds per cell. Hence, quantitative interpretations of these assays are severely limited.

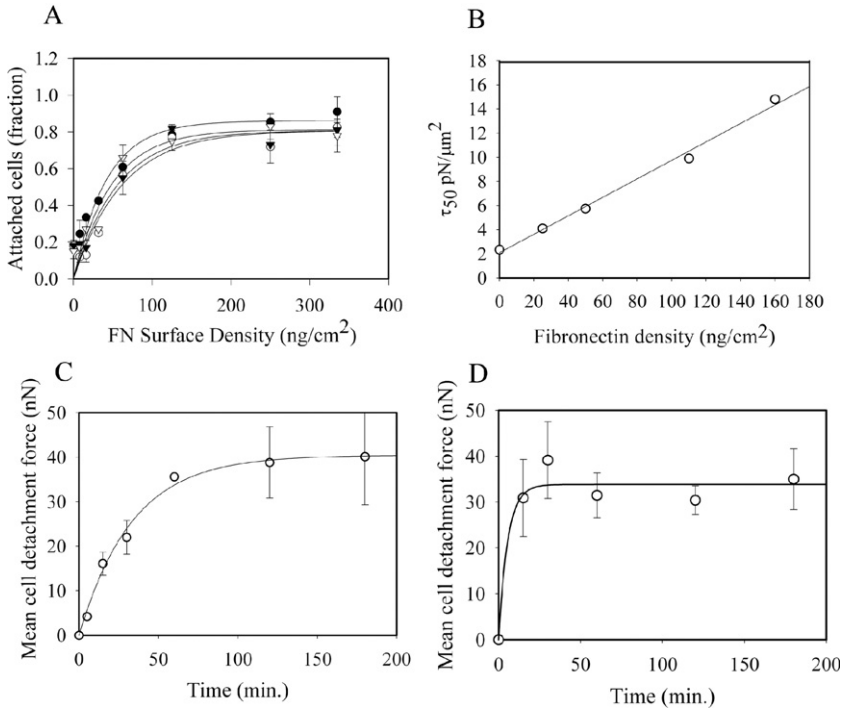

Figure 1. (A) Cell attachment assay for K562 cells plated on fibronectin for 60 min. (○) washed; (●) centrifuged 13 g; (▽) centrifuged 52 g; (▼) centrifuged 205 g. (B) Spinning disc analysis of K562 cells on different fibronectin densities showing mean cell detachment shear stress. t_{50} is the mean shear stress for cell detachment. (C) Spinning disc analysis of K562 cells on fibronectin (110 ng cm^{-2}) done at 20 °C and (D) spinning disc analysis of K562 cells on fibronectin (110 ng cm^{-2}) done at 37 °C. Both as a function of time and fit to the equation $y = a(1 - \exp(-bt))$, where a is the fit parameter for the plateau (40.4 and 33.8 nN), steady-state, b is the fit rate coefficient (0.03 and 0.18 min^{-1}), t is the time in minutes.

3.1.3. Quantitative measurement of the force required to detach cells. By controlling the force applied to cells, the mean force required to detach the cells can be measured. This can be done either as a bulk cell population or on an individual cell basis. Single cell force spectroscopy uses a modified atomic force microscope (AFM) to analyze cell detachment forces on an individual cell basis. This will be addressed both theoretically and experimentally below. First to give a background on our approach to the single cell force spectroscopy analyses, the bulk cell analysis method will be presented. The spinning disc method for analysis of cell adhesion has been developed over the past 12 years and >20 000 discs. It is based on a disc spinning in an infinite volume of fluid in which the hydrodynamic shear stress applied at the surface of the disc increases linearly with the distance from the axis of rotation. By measuring the proportion of cells detached as a function of radial position and fitting the data to a sigmoid curve, the mean shear stress for cell detachment can be measured and the force/cell calculated [18, 28]. Experimentally, the mean cell detachment force was proportional to the ligand density used and, hence, to the number of adhesive bonds expected under the law of mass action (figure 1(B)). This suggests that the cells detach by a single rupture cascade (discussed below).

The analysis of the $\alpha 5\beta 1$ integrin mediated adhesion of K562 cells to fibronectin using the spinning disc showed a linear dependence on ligand density with an extrapolation to zero fibronectin concentration showing a fibronectin independent component of (figure 1(B)). The kinetics of adhesion fit the expected (pseudo) first order kinetics expected for receptor–ligand binding in ligand excess, and is consistent with the law of mass action governing this reaction between tethered receptor and ligand as it would with the purified components (figures 1(C) and (D)). One limitation of the spinning disc approach is that it is difficult to make measurements at short adhesion times because of the delay in the settling of the cells on the substrate and the manipulations involved in the assay. Hence, the analysis for figure 1(C) was done at 20 °C to slow the reaction (rate constant = 0.030 min^{-1}). Running the reaction at 37 °C increased the rate to 0.18 min^{-1} at the expense of the early points on the curve (figure 1(D)). The values for the rate and steady-state levels for these reactions using the spinning disc provides a basis for expected values generated using single cell force spectroscopy with the CellHesion 200 system.

3.2. Biological issues for single cell force spectroscopy

Initial analyses using AFM were carried out using purified molecules and hence have avoided the complications introduced when whole cells are used in these measurements, Single cell force spectroscopy introduces a cell onto the AFM cantilever and requires a longer approach/retraction range to separate the cell from substrate during the retract phase [22]. Specialized instruments adapted to this analysis have become available commercially in recent years, making

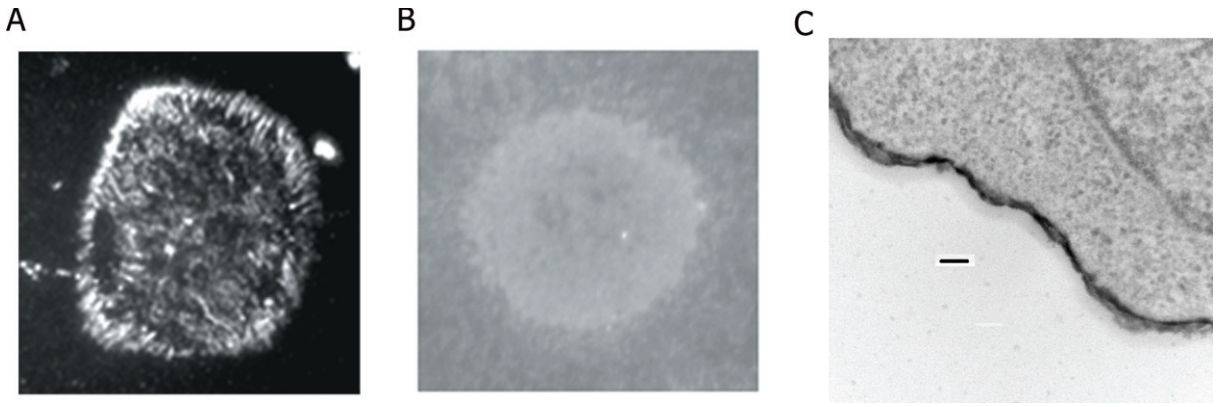

Figure 2. (A) HT1080 fibroblast at 90 min after plating, cell surface integrins were cross-linked to the fibronectin, cells were extracted and cross-linked $\beta 1$ integrin was stained. (B) K562 cells treated as in (A). (C) Transmission electron microscope picture of ruthenium red stained K562 cells at 100 000×. Dark stain is cell surface sugar (glycocalyx). Bar = 100 nm.

the experimental approach accessible to a wider range of researchers. Single cell force spectroscopy has been applied both to the measurement of single molecular bonds (reviewed recently [23]) and to cell adhesion involving multiple adhesive bonds [39]. It is important to consider the additional complications introduced by the use of intact cells.

3.2.1. Receptor clustering, complex formation, and signaling. As described above, integrins form clusters that nucleate large cytoplasmic protein complexes and connect the integrins to the actin cytoskeleton. This is also true for some other adhesion receptors such as cadherins [40]. These complexes may have a variety of effects on cell adhesion, but at this stage both their exact structure and functions are not well understood. It is possible that integrin must bind in clusters and form complexes to stabilize the adhesive bonds [27]. This would be consistent with the regulatory requirement that the integrin clusters and associated adhesion can be released through intracellular signals [41]. The attachment of the integrins to the actin cytoskeleton means that they can be tensioned by myosin II motors and this will trigger the catch bonds, at least for $\alpha 5\beta 1$ integrins [13, 42, 43]. In addition, signals transmitted through these complexes regulate the small G-proteins Rac and Rho, that in turn control the cytoskeletal structure and hence the tensioning of the adhesive bonds [44]. Given the complexity of these adhesive and regulatory controls, and our limited understanding of the functioning of the adhesive structures, it seems wise to remove these issues from the equation for the initial studies. Once we understand the other issues raised by the adhesive bonds, these can be addressed. One way to minimize these effects is to use a cell line that is defective in integrin clustering.

To minimize these issues in our experimental model, we have chosen to use K562 cells. These cells were derived from a CML (Chronic myelogenous leukemia) patient in blast crisis circulating in the blood [45]. They appear to represent a stage of hemopoietic development for which the cells should be confined to the bone marrow (i.e. adhering to the bone marrow stroma), so they have a presumptive adhesion defect. One consequence of this defect is their failure to form adhesion complexes and hence to generate adhesion mediated signals (compare the control adhesion labeled for substrate-bound $\alpha 5\beta 1$ integrin showing distinct clusters (figure 2(A)) with the K562 cells showing diffuse staining with no large clusters (figure 2(B))). The K562 cells appear not to be able to activate their cell surface adhesion receptor, $\alpha 5\beta 1$ integrin, which removes these issues from the experimental model. To activate the $\alpha 5\beta 1$ binding to fibronectin, either Mn^{++} is used instead of Mg^{++}, or activating antibodies are used (these antibodies capture the $\alpha 5\beta 1$ in the active state) [18].

3.2.2. Presence of multiple receptors. Cells generally express multiple adhesion receptors for binding to different ligands and even for binding to the same ligand. For example, there are eight integrin receptors that bind fibronectin and two of these, $\alpha v\beta 3$ and $\alpha 5\beta 1$ are often expressed together on cells in tissue culture. When multiple integrin receptors are expressed on the same cell there can be complex interactions that affect which receptor(s) are used for cell adhesion [46, 47]. In this report, using K562 cells simplifies this issue because they express only $\alpha 5\beta 1$ as an adhesion receptor.

3.2.3. Presence of a glycocalyx. Cells in multi-cellular animals are surrounded by a glycocalyx consisting of glycoproteins, glycolipids, proteoglycans, and polysaccharides that are bound to the cell surface and bound together by link proteins [40]. This glycocalyx can vary from 7 nm for red blood cells to several 100 nm for some epithelial and endothelial cells [48, 49]. Transmission electron microscopy stained with ruthenium red (dark stain) identifies a glycocalyx 40 ± 9.9 nm thick on K562 cells (figure 2(C)). Because the glycocalyx is mainly sugars, it is heavily hydrated. Transmission electron microscopy requires drying, so this is likely to be an underestimate of the true thickness. In contrast, integrins in their extended conformation (active) reach only 20 nm from the plasma membrane [50]. This has the important consequence that the first encounter of a cell lowered onto a substrate will be with the glycocalyx. Engaging the integrin will require either compressing or displacing the glycocalyx.

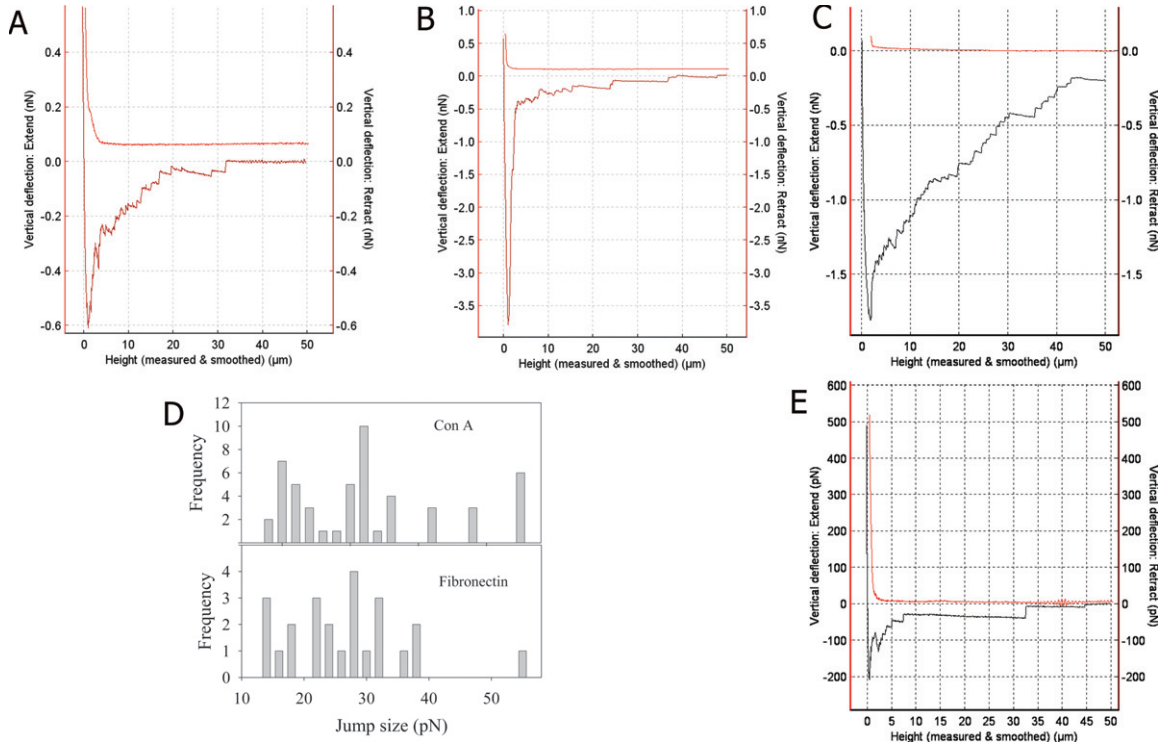

Figure 3. AFM analysis plots for K562 cells. The upper curve in each (ABCE) represents the approach curve and the lower is the retract curve. Height is the distance from the substrate surface. (A) Contact time 10 s on fibronectin; (B) same series contact time 40 s on fibronectin, (C) on concanavalin A substrate 180 s; (D) histogram distribution of jump sizes for the retract curve for concanavalin A (plot (C)) and fibronectin (plot (A)) showing the range of interactions. (E) Contact time 10 s on BSA.

For many cells in tissue culture, the thickness is 30–60 nm and displacement or reduction of glycocalyx thickness has been associated with sites of adhesion and increases in adhesion [51–53]. This principle is also used *in vivo* for adhesive regulation. The adhesive function of the neural cell adhesion molecule N-CAM is regulated physiologically by an increase in the addition of multiple sialic acid residues (sugars) to the extracellular domain of the protein [54]. Hence, the glycocalyx appears to serve an anti-adhesive rather than an adhesive function in some contexts. There is usually a relatively low level of non-specific binding of proteins and sugars [55]. However, the contact area between the cell and substrate can occupy several 100s μm^2/cell making some non-specific adhesion likely. Thus, these potential interactions of the cell and glycocalyx should be considered in cell adhesion measurements.

3.2.4. Cell viability. Cell viability is commonly determined using cell impermeant dyes which are either excluded from intact cells or loaded into cells in a cell permeant form and converted to an impermeant form by cellular enzymes. These measures of cell viability determine whether the plasma membrane is intact, and can exclude charged molecules. They could be useful to evaluate this during single cell force spectroscopy measurements. Since single cells are used for the assay, it is the viability of that cell which is important. In each approach–retract cycle of the AFM, it is possible that a portion of the cell or glycocalyx will be pulled from the cell surface, thus progressively changing the cell with each measurement. One approach to control this issue that has been used in single cell spectroscopy is to limit the number of measurements made with a single cell, in some protocols to as little as two or three, depending on the length of the contact time used [39]. We have taken an alternative approach in defining cell viability as the ability to retain the same cell adhesive response and hence have used repeated cycles of lengthening contact time and then compared the results to look for cycles where adhesive function fails.

3.3. Glycocalyx contributions to single cell force spectroscopy

All of the single cell force measurements reported generate retract curves that show the same features and are within the same quantitative range as published single cell force measurements [56–58]. What is different is the pattern of measurements and a different scientific perspective that is based on measurements made with other methods and the biological perspective on cell adhesion.

A typical series of measurements involved keeping the approach and retract rates at 5 $\mu m\ s^{-1}$, using a contact force of 0.5 nN and increasing contact times beginning with 5 s (figure 3(A)) increasing to 10, 20, 40 (figure 3(B)), 60 s. In this series, two portions of the retract curve can be observed: (i) a narrow peak close to the axis that represents F_{max} (maximum detachment force, or retract curve minimum) which increases as a function of time, and (ii) an extended series of

jumps forming a plot that extends 5–30 μm from the surface and shows little increase in magnitude with increased contact time. The strong narrow peak occurs within the first 5 μm of retraction and appears to detach as a single rupture cascade without intermediate jumps (figure 3(B)). Because this is the dominant peak and increases progressively with contact time, it was tentatively identified as due to integrin mediated adhesion. The expected properties of integrin mediated adhesion, based on our measurements with other methods and the structure of the adhering cell, are (i) that it increase with time on a seconds timescale (see figure 1(D)), and (ii) that the detachment will occur close to the origin. The reason for the latter is that integrins that form adhesive bonds also attach through their cytoplasmic domains to protein linkers that connect them mechanically to the actin cytoskeleton [13]. The bonds can then be tensioned by the myosin II mediated contraction of the actin filaments [59]. In cells spreading on a substrate, the integrins are not located at the leading edge of the cells but a short distance back from the edge [60]. In contrast, leukocytes in the circulating blood have plasma membranes that contain many invaginations and villi (protrusions), and selectins (adhesion receptors) are found on the tips of these villi [61]. The initial adhesion between leukocytes and the blood vessel wall is through the selectins, and during this interaction the force of the flowing blood on the cell causes membrane tethers to be drawn from the surface by the selectin bound to the vessel wall which acts as a brake to slow the movement of the cell driven by the flowing blood. This initiates rolling of the cell on the surface prior to formation of firm, integrin mediated adhesion to the vessel wall [62]. These tethers do not contain actin filaments. For these reasons, adhesion that is maintained at a distance from the origin in single cell force spectroscopy measurements is unlikely to be due to integrins.

To determine whether adhesion to the glycocalyx could generate the small jumps in the retract curve at distances up to 30 μm from the origin, the adhesive surface was coated with Concanavalin A (Con A) instead of fibronectin. Con A is a lectin that binds to α-mannosyl sugars and hence would pull on the glycocalyx directly (figure 3(C)). This retract curve show a series of jumps that extend at least 40 μm from the origin, demonstrating that the rupture of glycocalyx attachments can generate these distant rupture jumps. Note that $F_{\max}$ for the Con A substrate is larger than for the fibronectin substrate, as expected because of the higher number of bonds expected from the specific binding of Con A to the glycocalyx as opposed to the non-specific bonds between fibronectin and the glycocalyx. Treatment of cells with hyaluronidase to reduce the glycocalyx by the removal of hyaluronic acid and proteoglycans has been shown to increase adhesion of cells, due to a reduction of interference with integrin binding [51, 53]. Using single cell force spectroscopy, hyaluronidase treatment of cells reduced the average jump-size [63]. These observations are consistent with the jumps being the result of the breaking of glycocalyx linkages. If these jumps are due to non-specific interactions with the glycocalyx, then the size of the jumps would be variable (figure 3(D)). The exact composition, thickness, and materials properties of the glycocalyx will depend on many factors, including cell culture conditions and cell type. Hence, one does not expect to reproduce the exact pattern, but the multiple jumps and the distance from the origin is maintained. Using a BSA substrate to investigate non-specific adhesion also reveals a glycocalyx signature, but of smaller magnitude than on fibronectin in agreement with the higher charge concentrations in fibronectin (figure 3(E)). The very fine initial force spike suggests that there may be a suction component to the non-specific adhesion. A recent model suggests that the glycocalyx provides an essential anti-adhesive role in the regulation of cell adhesion and is essential for the generation of integrin clusters [27]. This is consistent with the fact that sugar-coated surfaces are generally resistant to formation of non-specific bonds with proteins [55, 57].

The specific adhesion due to the binding of integrins (and probably other adhesion receptor families) increases relatively slowly with time due to the reduced rate of diffusion of the receptors in the plasma membrane. In contrast, non-specific adhesion due to electrostatic interactions that occur randomly (not stereo-specific) over the surface increases little with time, except as the surface contact area may be increased due to cell spreading on the surface. Thus, the use of short contact times and weak contact forces increases the relative contribution of the non-specific glycocalyx mediated adhesion and reduces the contribution of the integrin mediated adhesion. The focus of many single cell force spectroscopy experiments on the measurement of single receptor–ligand bonds has the consequence that these short times are preferred because the probability of formation of multiple bonds increases with time [23]. While this is true for specific binding reactions, it is not clear that this will hold for non-specific bonds. While it is possible that some integrin engagements will be among the adhesive connections made at short times, it is unlikely that these will be the only adhesive connections that occur. The question is: what bonds are being measured? One can attempt to show specificity using inhibitors such as RGD peptides (but these are highly charged and are used at high concentrations), or antibodies (which attach to the surface and affect the glycocalyx interactions as well). Comparing two cell populations, one expressing and one not expressing the adhesion receptor, also would require an analysis of the glycocalyx as well to determine that it has not been altered. Thus, the problem of specificity when the whole cell is included is more complex than is generally reflected in the literature. The alternative hypothesis, to be disproven in the measurement of specific receptor mediated adhesion, is that the effects are not due to the glycocalyx.

3.4. Integrin contributions to single cell force spectroscopy

Single cell force spectroscopy provided a method to analyze single cells and to determine the variations of the rates of formation of adhesive integrin $\alpha5\beta1$-fibronectin bonds. First, it was necessary to establish the reproducibility of the measurements. To do this, cells were put through successive cycles of increasing contact time and $F_{\max}$ determined for each (figure 4(A)). Plotting the standard deviation and the variance for each time point showed that the variance gave a linear plot,

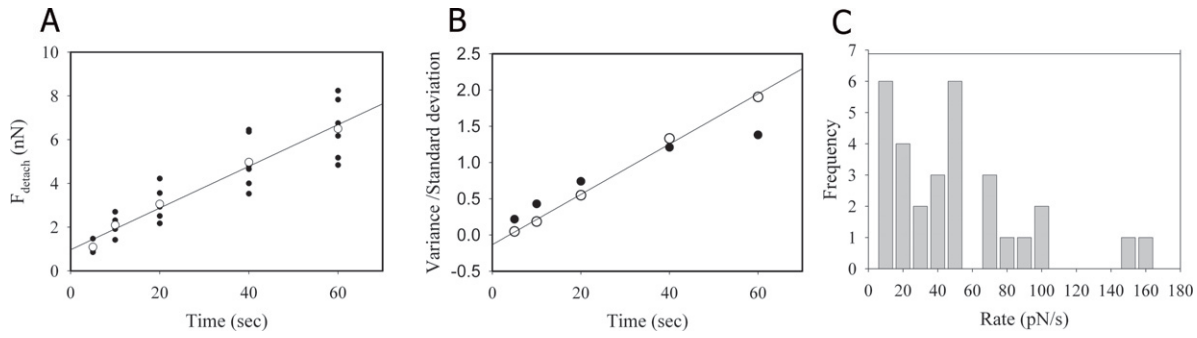

Figure 4. Analysis of responsive K562 cells adhesion rate. (A) Example of a single cell with six measurement cycles (●) with mean (○) and linear fit to the mean. (B) Standard deviation (●) and variance (○) for values shown in (A) with a linear fit to the variance ($R^2 = 0.996$). (C) Histogram distribution for 30 cells showing the distribution of rates. Data show a non-responsive group, peak at the left axis and a responsive peak that is spread with highest probability at 50 pN s^{-1} rise.

indicating that the individual values had a Gaussian distribution (figure 4(B)). The slopes of the plots of F_{max} versus time were determined by fitting to a linear equation. The distribution of these rates of increase in F_{max} showed a clustering in the 0–10 pN s^{-1} and the 40–50 pN s^{-1} ranges (figure 4(C)). The values in the 0–10 pN s^{-1} did not reach above the background and represent 20% of the cells. The remaining 80% showed varying rates of increase in adhesion. Interestingly, the simple wash assay also reached a plateau at 80%, indicating that 20% of the cell population was not able to adhere under the assay conditions (figure 1(A)). This is not because the cells were not viable, because the proportion of non-adhering cells can be increased by selection in culture. The remaining 80% had a broad distribution of rates of increase in F_{max}, with a mean of 75 pN s^{-1}. These can be compared to the spinning disc values. An increase of 75 pN s^{-1} gives a value of 4.5 nN at 1 min. Using the fit values for the plot in figure 1(D) ($y = a(1 - \exp(-bt))$, where $a = 33.8$ nN and $b = 0.18$ min^{-1}), gives a value of 5.6 nN at 1 min. Thus, the average rate of increase in detachment forces for the two methods provides a reasonably close fit to the first order rate equation with the same rate and plateau values.

These K562 cells show a broad distribution of rates of increase in F_{max}, which in turn is a reflection of the rates of increase in adhesive bonds in individual cells from 10 to 160 pN s^{-1}. We do not know why the distribution is so broad but both this variation and the existence of a non-adhering sub-population support the value of single cell analysis as opposed to pooling data from many cells to calculate averages. In these analyses, 2 cells were carried through the cycle of measurements (5, 10, 20, 40, 60 s) eight times for 40 measurements without a decrease in adhesive performance. In the analysis of successive cycles of measurement using the same cell, 50 comparisons were made. 24 showed an increase, 18 decreased and 8 remained the same in the following cycle. Hence, there is a weak trend to increase adhesion in successive cycles, which was evident particularly in the first 2–3 cycles of measurement. This may result from some loss of glycocalyx from the surface reducing the interference in later cycles.

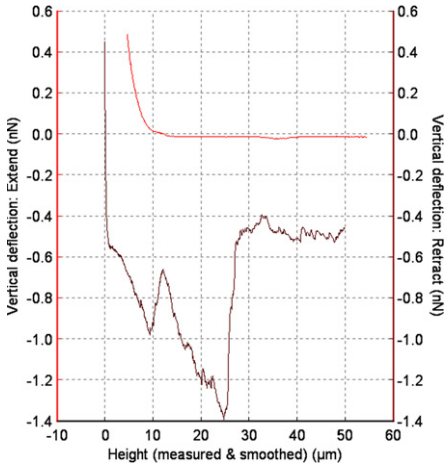

Figure 5. Soft cell. Approach and retract curves for a soft cell for 40 s contact time showing a broad distribution of detachment over the retraction distance. Compare with figure 2(B) showing the same time for a responsive cell from the same cell sample.

3.5. Force-induced cell detachment mechanism

The application of force to increase the rate of adhesive bond dissociation and subsequent cell detachment can generate two distinct forms of cell detachment. Cells can detach by a peeling mechanism that involves a series of discrete steps each involving the dissociation of a portion of the adhesive bonds that have the highest stress. In this mechanism the peak detachment force required will be less and the detachment will be distributed over a longer pulling range. In our analysis of K562 cells, an exceptional cell was observed that flattened more than others under compression and stretched like a soft balloon during retraction to a point where it was very elongated and held by two spots, one on the cantilever and one on the substrate, before final detachment from the substrate. The retract curve shows multiple peaks spread over 25 μm retraction, representing a peeling of the integrin bonds and finally a sharp step as the cell finally released from the substrate (figure 5). The F_{max} for this cell was only 1.4 nN at 40 s; much less than that for a stiff cell (figure 3(B)). This attachment–detachment was repeated three times, showing a similar retract

profile. The distinct difference in the retract curve with this cell, compared to the other cells tested, suggests that this is an example of the peeling detachment, whereas most cells detached by the alternative mechanism of a single rupture cascade. In the single rupture cascade, the force reaches a maximum at which the total adhesion fails. In the single cell force spectroscopy, that is seen in the F_{max} peak which occurs within 5 μm of the origin (figure 3(B)). We also believe that the cell detachment induced by the spinning disc occurs most often by a single rupture cascade, for two major reasons: (i) for MG63 cells the steady-state force required for cell detachment was 1084 nN/cell and the number of $\alpha5\beta1$ integrins available in the cell substrate interface was 4.8×10^4 giving a ratio of 23 pN per available integrin. Since the single bond analysis gives a value of 30–35 pN, there is little space for a sequential detachment mechanism; and (ii) through the analysis of many cell types, and several different integrins, a linear relationship has been observed between the mean force required for cell detachment and the ligand density [18–20, 64].

The actual mechanism of cell detachment will be influenced by several factors. As shown above, cell compliancy, presumably due to a reduced actin cytoskeleton, alters the force balance. Whether the force is applied at a specific point, as with micro-manipulation and micropipette methods, or whether the force is distributed broadly over the cell, as with hydrodynamic shear, affects the force balance. The $\alpha5\beta1$ integrin (at least) is a catch bond and requires a force to activate it to a more stable state [13, 38]. Detachment occurs from this more stable state, and to achieve this state requires that the integrin be attached to the actin cytoskeleton [13]. The actin cytoskeleton functions to redistribute forces [42, 65] and can be reinforced rapidly at a point of stress by cell responses to force [35, 66]. Thus, the cell is a complex mechanical object and force-induced detachment can occur by different mechanisms depending on the balance of forces and their distribution in the cell.

For determining the number of adhesive bonds represented by a specific cell detachment force, it is convenient if the cell detaches by a single rupture cascade and the measured force is the sum of the individual bond strengths. Then using an average single bond dissociation force at similar stress rates can be used to estimate the total number of adhesive bonds.

4. Summary and conclusions

All cells have a glycocalyx which contributes some non-specific adhesion between cells and their substrate. The effect of the glycocalyx is accentuated at very short adhesion times because the rate of binding of integrin–ligand adhesive bonds is slow and the non-specific binding is essentially independent of time. Importantly, the force signature of the glycocalyx adhesion could be distinguished from integrin mediated adhesion in the retract curves. The glycocalyx rupture occurred primarily at longer distances from the cell surface and was composed of many individual jumps in the retract curve. In contrast, the linkage of integrin to the actin cytoskeleton kept the integrin mediated rupture close to the origin and it detached in a single rupture cascade giving a single jump in most cases. The increase in F_{max} as a function of time reflected increases in the integrin mediated adhesion.

The experimental analysis used here employed a series of increasing contact times, at a relatively low contact force, to measure the rate of increase in adhesion, which would reflect an increase in the number of integrin–fibronectin adhesive bonds. The analysis of individual cells revealed that there were considerable differences in the rate of increase in adhesive bonds for the cells, and there was a sub-population that was non-adherent. Averaging the individual rates gave a value that is within the expected range for the rate of increase expected from the spinning disc analyses, showing that the two approaches give complementary measurements. The spinning disc analysis is based on large numbers of cells ($\sim$10 000 for each time point) and can exert large forces (in practice up to several μN's). This means it is useful for measuring the bulk quantities of the overall on- and off-rates for the adhesive bonds as well as the steady-state levels. Both the times required and the total forces used for those measurements are beyond the current practical capabilities for the single cell force spectroscopy measurements. Single force cell spectroscopy is much better for analysis of short times and analysis of the initial adhesive events which cannot be measured by the spinning disc method.

References

[1] Muller W E 1998 Origin of metazoa: sponges as living fossils *Naturwissenschaften* **85** 11–25

[2] Hynes R O and Zhao Q 2000 The evolution of cell adhesion *J. Cell Biol.* **150** F89–96

[3] Hynes R O 1994 Genetic analyses of cell-matrix interactions in development *Curr. Opin. Genetics Dev.* **4** 569–74

[4] Shattil S J and Newman P J 2004 Integrins: dynamic scaffolds for adhesion and signaling in platelets *Blood* **104** 1606–15

[5] Wiseman P W *et al* 2004 Spatial mapping of integrin interactions and dynamics during cell migration by image correlation microscopy *J. Cell Sci.* **117** 5521–34

[6] Shattil S J and Ginsberg M H 1997 Integrin signaling in vascular biology *J. Clin Invest.* **100** S91–5

[7] Ginsberg M H, Du X and Plow E F 1992 Inside-out integrin signalling *Curr. Opin. Cell Biol.* **4** 766–71

[8] Takagi J, Petre B M, Walz T and Springer T A 2002 Global conformational rearrangements in integrin extracellular domains in outside-in and inside-out signaling *Cell* **110** 599–11

[9] Hynes R O 2002 Integrins: bidirectional, allosteric signaling machines *Cell* **110** 673–87

[10] Ye F *et al* 2010 Recreation of the terminal events in physiological integrin activation *J. Cell Biol.* **188** 157–73

[11] Anthis N J *et al* 2009 Beta integrin tyrosine phosphorylation is a conserved mechanism for regulating talin-induced integrin activation *J. Biol. Chem.* **284** 36700–10

[12] Menko A S and Boettiger D 1987 Occupation of the extracellular matrix receptor, integrin, is a control point for myogenic differentiation *Cell* **51** 51–7

[13] Friedland J C, Lee M H and Boettiger D 2009 Mechanically activated integrin switch controls $\alpha_5\beta_1$ function *Science* **323** 642–4

[14] Miranti C K and Brugge J S 2002 Sensing the environment: a historical perspective on integrin signal transduction *Nat. Cell Biol.* **4** E83–90

[15] Schwartz M A and Horwitz A R 2006 Integrating adhesion, protrusion, and contraction during cell migration *Cell* **125** 1223–5

[16] Pierschbacher M D, Hayman E G and Ruoslahti E 1983 Synthetic peptide with cell attachment activity of fibronectin *Proc. Natl Acad. Sci. USA* **80** 1224–7
[17] Lotz M M, Burdsal C A, Erickson H P and McClay D R 1989 Cell adhesion to fibronectin and tenascin: quantitative measurements of initial binding and subsequent strengthening response *J. Cell Biol.* **109** 1795–805
[18] Garcia A J, Huber F and Boettiger D 1998 Force required to break alpha5beta1 integrin–fibronectin bonds in intact adherent cells is sensitive to integrin activation state *J. Biol. Chem.* **273** 10988–93
[19] Shi Q and Boettiger D 2003 A novel mode for integrin-mediated signaling: tethering is required for phosphorylation of FAK Y397 *Mol. Biol. Cell* **14** 4306–15
[20] Boettiger D 2007 Quantitative measurements of integrin-mediated adhesion to extracellular matrix *Methods Enzymol.* **426** 1–25
[21] Weisel J W, Shuman H and Litvinov R I 2003 Protein–protein unbinding induced by force: single-molecule studies *Curr. Opin. Struct. Biol.* **13** 227–35
[22] Benoit M, Gabriel D, Gerisch G and Gaub H E 2000 Discrete interactions in cell adhesion measured by single-molecule force spectroscopy *Nat. Cell Biol.* **2** 313–7
[23] Helenius J, Heisenberg C P, Gaub H E and Muller D J 2008 Single-cell force spectroscopy *J. Cell Sci.* **121** 1785–91
[24] Duband J-L *et al* 1988 Fibronectin receptor exhibits high lateral mobility in embryonic locomoting cells but is immobile in focal contacts and fibrillar streaks in stationary cells *J. Cell Biol.* **107** 1385–96
[25] Cluzel C, Saltel F, Lussi J, Paulhe F, Imhof B A and Wehrle-Haller B 2005 The mechanisms and dynamics of $\alpha v\beta 3$ integrin clustering in living cells *J. Cell Biol.* **171** 383–92
[26] Burridge K and Chrzanowska-Wodnicka M 1996 Focal adhesions, contractility, and signaling *Annu. Rev. Cell Dev. Biol.* **12** 463–518
[27] Paszek M J, Boettiger D, Weaver V M and Hammer D A 2009 Integrin clustering is driven by mechanical resistance from the glycocalyx and the substrate *PLoS Comput. Biol.* **5** e1000604
[28] Truskey G A and Proulx T L 1993 Relationship between 3T3 cell spreading and the strength of adhesion on glass and silane surfaces *Biomaterials* **14** 243–54
[29] Cox S M, Baur P S and Haenelt B 1977 Retention of the glycocalyx after cell detachment by EGTA *J. Histochem. Cytochem.* **25** 1368–72
[30] Chen W-T, Wang J, Hasegawa T, Yamada S S and Yamada K M 1986 Regulation of fibronectin receptor distribution by transformation, exogenous fibronectin, and synthetic peptides *J. Cell Biol.* **103** 1649–61
[31] Harris A 1973 Location of cellular adhesions to solid substrata *Dev. Biol.* **35** 97–114
[32] Horwitz A F, Duggan K, Buck C A, Beckerle M C and Burridge K 1986 Interaction of plasma membrane fibronectin receptor with talin—a transmembrane linkage *Nature* **320** 531–3
[33] Zamir E and Geiger B 2001 Components of cell-matrix adhesions *J. Cell Sci.* **114** 3577–9
[34] Zamir E and Geiger B 2001 Molecular complexity and dynamics of cell-matrix adhesions *J. Cell Sci.* **114** 3583–90
[35] Riveline D *et al* 2001 Focal contacts as mechanosensors: externally applied local mechanical force induces growth of focal contacts by an mDia1-dependent and ROCK-independent mechanism *J. Cell Biol.* **153** 1175–86
[36] Ballestrem C, Hinz B, Imhof B A and Wehrle-Haller B 2001 Marching at the front and dragging behind: differential $\alpha V\beta 3$-integrin turnover regulates focal adhesion behavior *J. Cell Biol.* **155** 1319–32
[37] Humphries M J 1998 Cell adhesion *Current Protocols in Cell Biology* ed J S Bonifacino, M Dasso, J B Harford, J Lippincott-Schwartz and K M Yamada (New York: Wiley) pp 9.1.1–.11
[38] Kong F, Garcia A J, Mould A P, Humphries M J and Zhu C 2009 Demonstration of catch bonds between an integrin and its ligand *J. Cell Biol.* **185** 1275–84
[39] Franz C M, Taubenberger A, Puech P H and Muller D J 2007 Studying integrin-mediated cell adhesion at the single-molecule level using AFM force spectroscopy *Sci STKE* **2007** l5
[40] Alberts B, Johnson A, Lewis J, Raff M, Roberts K and Walter P 2002 *Molecular Biology of the Cell* 4th edn (New York: Garland Science)
[41] Li S, Guan J L and Chien S 2005 Biochemistry and biomechanics of cell motility *Annu. Rev. Biomed. Eng.* **7** 105–50
[42] Cai Y *et al* 2010 Cytoskeletal coherence requires myosin-IIA contractility *J. Cell Sci.* **123** 413–23
[43] Vicente-Manzanares M, Zareno J, Whitmore L, Choi C K and Horwitz A F 2007 Regulation of protrusion, adhesion dynamics, and polarity by myosins IIA and IIB in migrating cells *J. Cell Biol.* **176** 573–80
[44] Burridge K and Wennerberg K 2004 Rho and Rac take center stage *Cell* **116** 167–79
[45] Klein E *et al* 1976 Properties of the K562 cell line, derived from a patient with chronic myeloid leukemia *Int. J. Cancer* **18** 421–31
[46] Calderwood D A, Tai V, Di P G, De C P and Ginsberg M H 2004 Competition for talin results in trans-dominant inhibition of integrin activation *J. Biol. Chem.* **279** 28889–95
[47] Caswell P T, Chan M, Lindsay A J, McCaffrey M W, Boettiger D and Norman J C 2008 Rab-coupling protein coordinates recycling of alpha5beta1 integrin and EGFR1 to promote cell migration in 3D microenvironments *J. Cell Biol.* **183** 143–55
[48] Ito S 1969 Structure and function of the glycocalyx *Fed Proc.* **28** 12–25
[49] Martins M F and Bairos V A 2002 Glycocalyx of lung epithelial cells *Int. Rev. Cytol.* **216** 131–73
[50] Xiong J P *et al* 2002 Crystal structure of the extracellular segment of integrin $\alpha V\beta 3$ in complex with an Arg–Gly–Asp ligand *Science* **296** 151–5
[51] Soler M *et al* 1998 Adhesion-related glycocalyx study: quantitative approach with imaging-spectrum in the energy filtering transmission electron microscope (EFTEM) *FEBS Lett.* **429** 89–94
[52] Sabri S, Soler M, Foa C, Pierres A, Benoliel A and Bongrand P 2000 Glycocalyx modulation is a physiological means of regulating cell adhesion *J. Cell Sci.* **113** 1589–600
[53] Datta A, Shi Q and Boettiger D E 2001 Transformation of chicken embryo fibroblasts by v-src uncouples beta1 integrin-mediated outside-in but not inside-out signaling *Mol. Cell Biol.* **21** 7295–306
[54] Sorribas H, Braun D, Leder L, Sonderegger P and Tiefenauer L 2001 Adhesion proteins for a tight neuron-electrode contact *J. Neurosci. Methods* **104** 133–41
[55] Lee M H, Boettiger D and Composto R J 2008 Biomimetic carbohydrate substrates of tunable properties using immobilized dextran hydrogels *Biomacromolecules* **9** 2315–21
[56] Taubenberger A, Cisneros D A, Friedrichs J, Puech P H, Muller D J and Franz C M 2007 Revealing early steps of $\alpha_2\beta_1$ integrin-mediated adhesion to collagen type I by using single-cell force spectroscopy *Mol. Biol. Cell* **18** 1634–44
[57] Puech P H, Taubenberger A, Ulrich F, Krieg M, Muller D J and Heisenberg C P 2005 Measuring cell adhesion forces of primary gastrulating cells from zebrafish using atomic force microscopy *J. Cell Sci.* **118** 4199–206

[58] Fierro F A *et al* 2008 BCR/ABL expression of myeloid progenitors increases beta1-integrin mediated adhesion to stromal cells *J. Mol. Biol.* **377** 1082–93
[59] Conti M A and Adelstein R S 2008 Nonmuscle myosin II moves in new directions *J. Cell Sci.* **121** 11–8
[60] Hu K, Ji L, Applegate K T, Danuser G and Waterman-Storer C M 2007 Differential transmission of actin motion within focal adhesions *Science* **315** 111–5
[61] Galkina S I, Molotkovsky J G, Ullrich V and Sud'ina G F 2005 Scanning electron microscopy study of neutrophil membrane tubulovesicular extensions (cytonemes) and their role in anchoring, aggregation and phagocytosis. The effect of nitric oxide *Exp. Cell Res.* **304** 620–9
[62] Edmondson K E, Denney W S and Diamond S L 2005 Neutrophil-bead collision assay: pharmacologically induced changes in membrane mechanics regulate the PSGL-1/P-selectin adhesion lifetime *Biophys. J.* **89** 3603–14
[63] Sun M *et al* 2005 Multiple membrane tethers probed by atomic force microscopy *Biophys. J.* **89** 4320–9
[64] Boettiger D, Lynch L, Blystone S and Huber F 2001 Distinct ligand-binding modes for integrin alpha(v)beta(3)-mediated adhesion to fibronectin versus vitronectin *J. Biol. Chem.* **276** 31684–90
[65] Maniotis A J, Chen C S and Ingber D E 1997 Demonstration of mechanical connections between integrins, cytoskeletal filaments, and nucleoplasm that stabilize nuclear structure *Proc. Natl Acad. Sci. USA* **94** 850–4
[66] Choquet D, Felsenfield D P and Sheetz M P 1997 Extracellular matrix rigidity causes strengthening of integrin-cytoskeletal linkages *Cell* **88** 39–48